

NUMERICAL MODELLING OF FRP PLATE REINFORCED GLULAM

Gary Raftery¹, Annette Harte²

ABSTRACT: Low-grade glued laminated timber (glulam) can be effectively reinforced using fibre reinforced polymer (FRP) materials. This paper discusses the development and application of a nonlinear finite element model to simulate the behaviour of unreinforced and FRP plate reinforced low-grade glulam beams. The model utilises constitutive relationships developed from mechanical testing of the timber. Anisotropic plasticity theory is employed in the model and the failure model is the maximum stress criterion. The predicted behaviour agrees strongly with experimental findings for load-deflection, stiffness and ultimate moment capacity of the unreinforced and reinforced beams. A parametric analysis demonstrated that as the FRP reinforcement percentage was increased, enhancements in the stiffness, ultimate moment capacity and nonlinear behaviour of the hybrid beam could be obtained.

KEYWORDS: Finite element modelling, Glued laminated timber, Fibre reinforced polymers, Composites, Ductility

1 INTRODUCTION

Timber is well accepted as a material by structural engineers. Its use has many benefits in the construction industry. It is natural, renewable, and sustainable [1]. It is of low cost, is versatile, has excellent strength to weight properties and is aesthetically pleasing. In recent times, fibre reinforced polymers have emerged as useful materials in the construction industry. These materials are regularly employed for strengthening and upgrading existing concrete structures [2]. They have many advantages. They have excellent mechanical properties, are lightweight and are non-corrosive. In addition, these materials can be manufactured in factory controlled environments to very precise tolerances in relation to their mechanical properties. With increased focus being placed on promoting timber as an environmentally friendly material, experimental research was undertaken into the use of FRP plate to reinforce in flexure low-grade glulam [3]. Plate reinforcement is more compatible with the glulam manufacturing process although the use of bonded-in rods has also achieved favourable results [4]. When modest FRP reinforcement percentages are strategically located in the higher stressed tension zones of the glulam beams, reasonable improvements in the

stiffness and more significant improvements in the ultimate moment capacity can result in comparison to the performance of unreinforced beams. Furthermore, the FRP reinforced beams are associated with ductile behaviour in comparison to the brittle tension failures experienced by the unreinforced beams. Numerical modelling is a useful tool for the optimisation of structural components such as FRP reinforced glulam. If experimental behaviour can be simulated to a satisfactory level of precision using a numerical model, then the cost associated with extensive test programmes can be reduced and further behaviour of the reinforced beams can be studied using a numerical approach.

1.1 OBJECTIVES

This paper focuses on the development of a non-linear numerical model that could accurately simulate the mechanical behaviour of unreinforced and FRP reinforced low-grade glulam during static loading. The finite element programme ANSYS was employed for the simulations. Accurate predictions of load-deflection behaviour, stiffness and ultimate moment capacity are required. In order to do this, a programme of material characterisation studies was undertaken to determine relationships and properties for the timber and material properties for the FRP which could be used as input data for the model. The test programmes involved the following:

- (i) Compression testing of in-grade timber.
- (ii) Tension testing of in-grade timber.
- (iii) Density variability study of in-grade timber.
- (iv) Tension testing of FRP.

¹ Gary Raftery, Civil Engineering, College of Engineering and Informatics, National University of Ireland, Galway, University Road, Galway, Ireland. Email:

Gary.Raftery@nuigalway.ie

² Annette Harte, Civil Engineering, College of Engineering and Informatics, National University of Ireland, Galway, University Road, Galway, Ireland. Email: Annette.Harte@nuigalway.ie

2 NUMERICAL MODELLING

A finite element model was developed to simulate the behaviour of FRP reinforced (Phase B) and unreinforced glulam beams (Phase A) which were loaded in four-point bending. The test arrangement for the unreinforced and reinforced beams is shown in Figure 1. The span and overall length of each of the beams was 3420mm and 3610mm, respectively. The loading arrangements correspond with the recommended test procedures stated in EN 408 [5].

The glulam beams were manufactured from mechanically graded C16 Sitka spruce laminations. Five laminations 96mm wide and 38mm deep were glued together using a PRF adhesive to produce a section 96mm wide and 190mm deep. The reinforced beams comprised the same 190mm deep glulam beams with an FRP plate bonded to the soffit with an epoxy adhesive. The FRP reinforcement comprised unidirectional glass-fibres in an engineered thermoplastic polyurethane matrix (Fulcrum). Two 1.2mm thick Fulcrum plates were adhesively bonded together to form an overall plate 96mm wide and 2.8mm thick. This gives a reinforcement

percentage of approximately 1.26% for the 190mm deep glulam beams. The configurations for the unreinforced and reinforced beams are illustrated in Figure 2.

A two-dimensional finite element model for these beams was developed using the commercial FE package ANSYS. Due to symmetry, it was only necessary to model half of the beam as shown in Figure 3. The end support was modelled as a roller support to permit translation of the beam in the longitudinal direction. Separate entities were created for each lamination so that the material characteristics of the individual laminations could be incorporated in the model. As no bondline failures in the glulam beams were observed during testing, the PRF adhesive between the laminations was not included in the model and a perfect connection was assumed to exist. Perfect connections were assumed to exist at the epoxy/wood interface and the epoxy/FRP interface as excellent quality bonds were obtained between this adhesive, the FRP type and the wood in a previous experimental study [6]. The model also includes steel plates at the loading and support points in order to avoid stress concentrations at these locations.

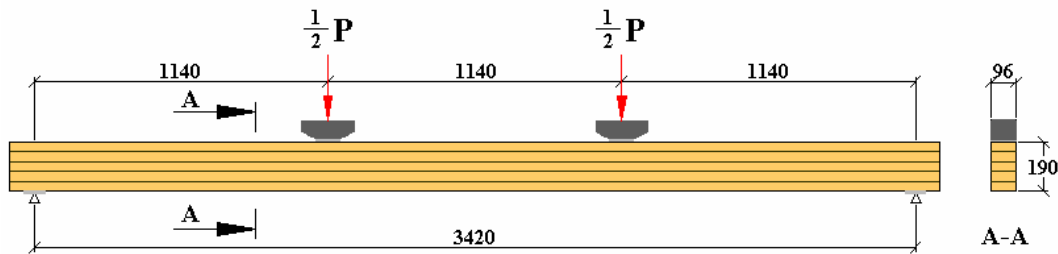


Figure 1: Failure test arrangement for unreinforced and FRP plate reinforced glulam beams

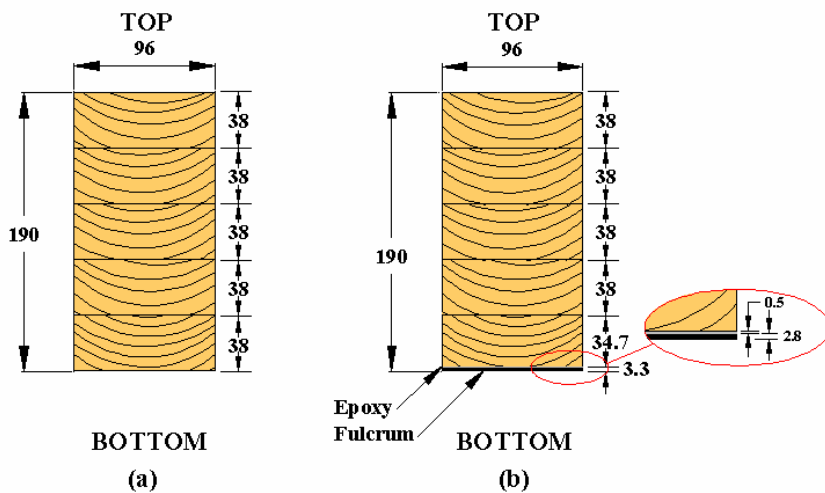


Figure 2: Beam Configurations: (a) Unreinforced glulam (b) FRP plate reinforced glulam

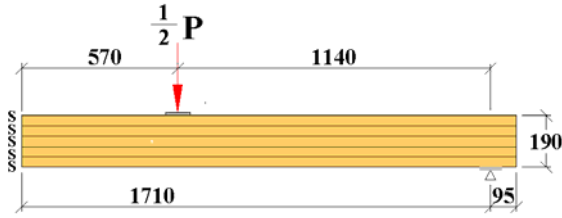


Figure 3: Geometrical arrangement for FE model

The elements used were 8-noded second-order plane-stress elements (Plane 82) having plasticity and large deflection capabilities. A mesh discretisation study was carried out to determine a suitable element size and the resulting finite element mesh is shown in Figure 4 for the unreinforced beams and in Figure 5 for the reinforced beams. Two elements were used through the thickness of each lamination. For the FRP reinforcement and the 0.5mm thick epoxy adhesive layer, one element was used through the thickness in each case.

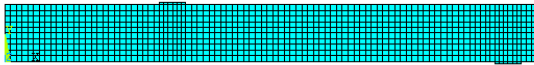


Figure 4: FE mesh for unreinforced beams

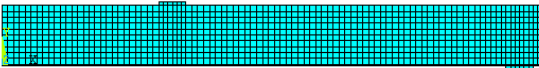


Figure 5: FE mesh for reinforced beams

The use of appropriate constitutive models for each material is essential if accurate predictions of structural performance are to be achieved. Unreinforced timber glulam beams usually fail in tension before any plasticity has developed on the compression face so linear elastic models suffice. However, this is not the case for reinforced glulams where, depending on the level of reinforcement, significant plasticity can occur. The stress-strain behaviour used to model the timber parallel to grain is illustrated in Figure 6. A linear elastic, perfectly plastic material model was employed for the behaviour of the timber parallel to grain in compression while a linear elastic brittle material model is employed for timber in tension. The ultimate tensile strength, f_{Ly}^t occurs at a strain, ϵ_L^t . The ultimate compressive strength f_{Ly}^c occurs at a strain, ϵ_L^c and perfect plastic behaviour occurs in the longitudinal direction of the timber after this strain value. The tension stress along the longitudinal axis is represented by σ_L^t and the compressive stress along the longitudinal axis is represented by σ_L^c .

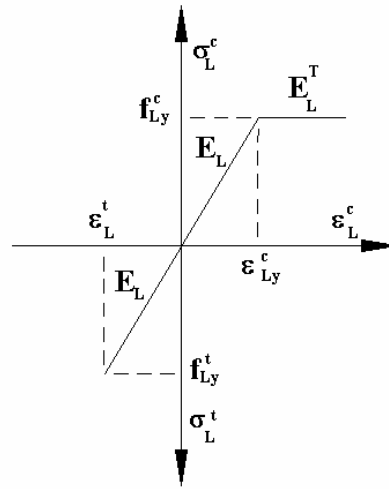


Figure 6: Stress-strain behaviour of timber parallel to grain

ANSYS incorporates material models based on the theory of anisotropic plasticity. This theory was employed in the model to include the plastic behaviour of the timber in the top two laminations in the compression zone. The theory includes bi-linear behaviour for the timber in the three orthogonal directions as well as the three shear planes. Therefore, normal compressive yield stresses are declared for the longitudinal, f_{Ly}^c , radial, f_{Ry}^c and tangential, f_{Ty}^c directions as well as yield shear stresses in the three planes. Tangent moduli, E^T or tangent shear moduli, G^T define the behaviour of the material after yielding. For the radial and tangential directions, the elastic-plastic responses for the timber in compression are shown in Figure 7 (a) and (b), respectively. These models require the specification of a large number of material parameters for the timber. The characterisation studies to determine the required values for the timber in tension and compression parallel to grain are described below. The characterisation of the other materials is more straightforward. The FRP plate is modelled as a linear elastic orthotropic material, and the adhesive and steel are treated as linear elastic isotropic materials.

A static small displacement analysis was undertaken, whereby a series of displacement-controlled increments were applied at the loading plate during which convergence was obtained. The midspan deflection and the reaction force were recorded for every increment. Failure in the model was based on the maximum stress criterion whereby the model was programmed to deactivate elements when the tension stresses in the longitudinal direction, at a displacement step, reached the critical tension failure strengths of the timber laminations. A parametric analysis was also undertaken using the finite element model, which investigated the effect of varying the reinforcement percentage of the FRP material. This study involved examining the FRP plate with a variety of reinforcement thicknesses.

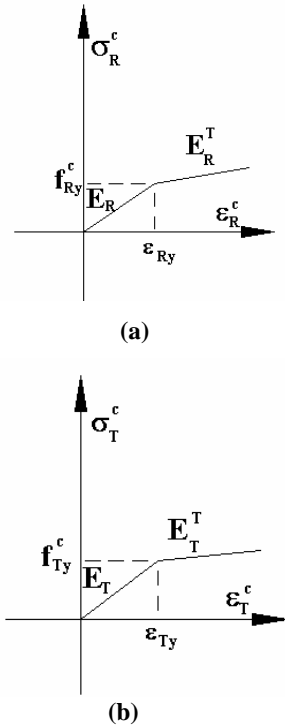


Figure 7: Elastic-plastic stress-strain relationships (a) radial direction (b) tangential direction.

3 MATERIAL CHARACTERISATION

Material characterisation for the finite element model was undertaken using experimental test programmes, well established relationships and published data. The experimental test programmes involved the testing of in-grade timber specimens in tension and in compression, the assessment of the variability in the density of the timber and the testing of the FRP material in tension.

3.1 COMPRESSION TESTING OF TIMBER

Eighty-two in-grade specimens of Irish grown Sitka spruce were tested parallel to grain using the Denison testing machine according to EN 408 [5]. Test specimens were selected such that the critical strength reducing knot area ratios in the section were located in the centre of the test specimen. Each test specimen had a thickness of 38mm and width of 96mm which coincided with the lamination size employed in the manufacture of the glulam beams. The corresponding lengths of the test specimens were 226mm in accordance with EN 408. Specimens were initially conditioned in an environment of $65 \pm 5\%$ relative humidity and a temperature of $20 \pm 2^\circ\text{C}$. The loading faces of the test pieces were sanded smooth and square. Each test piece was positioned parallel to the axis of the loading machine so that no eccentricity existed and a preload of 1.5kN was applied. Load was applied at a constant loading-head movement rate so that the maximum load was obtained within $300 \pm 120\text{s}$. The ultimate compressive strength of each specimen was determined by dividing the maximum load by the cross-sectional area. The corresponding density of each piece was determined by cutting a specimen 40mm

in length from the section which was free of knots or other features such as resin pockets which were non-representative of the timber. The moisture content of the timber was determined by the oven drying procedure and the knot area was recorded with reference to IS 127 [7]. The results from the compression testing of the in-grade samples of timber are shown in Figure 8, where the compression strength at failure is plotted against the knot area ratio and in Figure 9, where the compression strength at failure is plotted against density measurements from the samples.

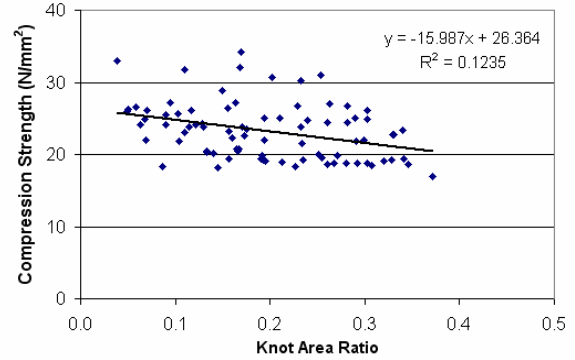


Figure 8: In-grade timber compressive strength versus knot area ratio

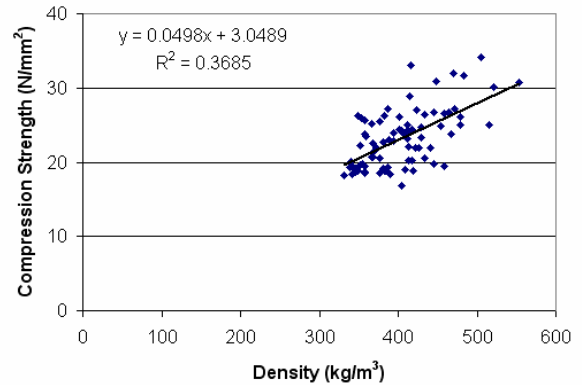


Figure 9: In-grade timber compression strength versus density

A multiple regression analysis where density and knot area ratio were employed as independent variables to predict the ultimate compressive strength of in-grade Irish grown Sitka spruce obtained a coefficient of multiple determination of 0.503. The multiple regression relationship is expressed in Equation 1.

$$f_{Ly}^c = 6.03 + 0.0506(\rho_w) - 16.7(KAR) \quad (1)$$

where f_{Ly}^c is the ultimate compression strength of the timber parallel to grain, ρ_w is the density of the wood, KAR is the knot area ratio.

3.2 TENSION TESTING OF TIMBER

The in-grade timber tension test programme involved testing parallel to grain specimens to determine the failure strength in accordance with the procedures specified in EN 408 [5]. Eighty-three specimens were tested. The test pieces were carefully selected from 4200mm long boards so that the most critical knot area ratio was included. The pieces were conditioned in an environment of 65±5% relative humidity and a temperature of 20±2°C for twenty days prior to testing. The total knot area ratio was measured with reference to IS 127 [7]. The specimens tested were a minimum 1600mm in length which ensured a free length of 1000mm from the end grips. A constant rate of crosshead movement was applied so that failure in the specimens occurred in 300±120 seconds. The ultimate strength was determined by dividing the failure load by the cross-sectional dimensions which were measured using a vernier caliper that had a precision of 0.01mm. Density specimens of approximate length of 30mm and cross-sectional area of the specimen were taken from beside the location of the fracture.

The results of the in-grade timber tension testing programme are shown by means of a plot of tensile strength versus total knot area ratio in Figure 10 where a correlation coefficient of 0.3867 was obtained.

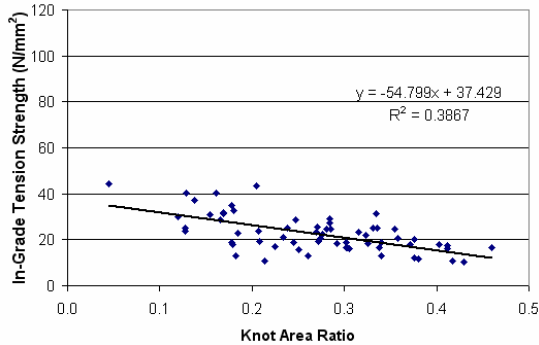


Figure 10: In-grade timber tension strength versus knot area ratio

Density was found to have little influence on the tensile strength of the timber. By recording the knot area ratio of the tension laminations in the beams, an estimate of their strength could therefore be obtained. The laminating effect which is the increase in strength of a timber lamination when bonded in a glulam beam in comparison to when tested in a uniaxial test was accounted for prior to entering the estimated failure strength data for the timber into the nonlinear numerical model code. Falk et al. [8] reported a value of 1.26 for the laminating effect for a beam made of homogeneous C30 grade laminations. Use of higher grade C37 laminations resulted in a significantly lower laminating factors [9]. Hence, the application of 1.26 to the tensile strength of the C16 grade laminations is conservative.

3.3 DENSITY VARIABILITY STUDY

An examination of the variability in the density of samples along a number of laminations was also necessary in order to maintain a practical approach to determine the density of the wood in the laminations. If density proved influential on the strength of the timber and if fluctuations in the density of the wood in the laminations were considered to be insignificant, an estimate of the density could be obtained using density data from the ends of laminations. Six boards of timber were examined. The boards were of a cross-section of 96mm x 44mm and were 4200mm long. The boards were conditioned to an environment of 65±5% relative humidity and a temperature of 20±2°C to an approximate equilibrium moisture content of 12% moisture content. Specimens 50mm in thickness and of the cross-sectional area of the board were cut at regular intervals such that only clear wood that was free of knots and defects was selected. The wood samples were weighed using a mass balance with precision to 0.01g. The dimensions of the specimens were measured using a vernier caliper with precision to 0.01mm. The density of each piece was determined from the recorded measurements. The moisture content of the specimens was determined by the oven drying procedure.

The mean and standard deviation of the density variability results as well as the number of samples taken along the 4200mm board length can be seen in Table 1. The deviations between the readings for all six boards are not deemed to be significant. Therefore, it was considered appropriate that the clear density of each lamination could be determined from cutting a specimen at the end of each board. For the finite element model, the ultimate compressive strength of the timber laminations at the top of the beam could therefore be estimated from readings of the maximum knot area ratio and the measurements of density taken from the cut-offs.

Table 1: Variability of density

Board	Number of specimens	Density (kg/m ³)	St. Dev.
1	14	387	14
2	11	410	19
3	8	363	14
4	15	350	11
5	18	399	12
6	15	394	17

3.4 BENDING STIFFNESS

A mechanical stress grading machine was used to evaluate the modulus of elasticity in bending at intervals along each lamination. A global modulus of elasticity was determined for each lamination using the local readings.

3.5 PUBLISHED DATA/ESTABLISHED RELATIONSHIPS

The remaining parameters for the timber were determined from a combination of established relationships and published data. While considerable variation is associated with the mechanical properties in wood, the relationship between the Young's moduli in the three timber orientations expressed by Bodig and Jane [10] in Equation 2 and the relationship between the three shear moduli as expressed in Equation 3 were applied to the timber in the model.

$$E_L:E_R:E_T \approx 20:1.6:1 \quad (2)$$

$$G_{LR}:G_{LT}:G_{RT} \approx 10:9.4:1 \quad (3)$$

where, E_L, E_R, E_T are the Young's moduli in the longitudinal, radial and tangential directions and G_{LR}, G_{LT}, G_{RT} are the shear moduli in the respective planes. The relationship between E_L and G_{LR} as expressed in Equation 4 [10] was also used.

$$E_L:G_{LR} \approx 14:1 \quad (4)$$

Poisson's ratio values of 0.37, 0.47 and 0.43 for ν_{LR}, ν_{LT} and ν_{RT} , respectively, were employed in the finite element model are given for Sitka spruce [11]. The relationships and sources of data used for the moduli of elasticity E , tangent moduli E^T , and the yield stresses f_y , in the three orthogonal directions are shown in Table 2. Axes orientation is illustrated in relation to the grain direction in the timber. Elastic-plastic stress-strain data was also inputted for the three shear planes as shown in Table 3.

Table 2: Elastic-plastic properties of the timber in compression for the three orthogonal axes

Axes	E ($N/mm^2 \times 10^3$)	E^T ($N/mm^2 \times 10^3$)	f_y (N/mm^2)
L	[a]	0	[b]
R	[c]	30 [d]	5.3 [d]
T	[c]	25 [d]	5.6 [d]

KEY:

- Mechanical stress grading results
- Material characterisation testing
- Equation 2 [10]
- [4]

Table 3: Elastic-plastic properties of the timber in compression for the three shear planes

Axes	G ($N/mm^2 \times 10^3$)	G^T ($N/mm^2 \times 10^3$)	τ_y (N/mm^2)
LR	[e]	0 [d]	11 [d]
RT	[f]	0 [d]	11 [d]
LT	[f]	0 [d]	8 [d]

KEY:

- [4]
- Equation 4 [10]
- Equation 3 [10]

3.6 TENSION TESTING OF FRP

The FRP material was tested in tension with reference to EN 2747 [12] in order to determine its tensile modulus of elasticity and tensile strength. Tests were carried out for 2.8mm thick FRP plate (two plates of 1.2mm bonded together with epoxy adhesive) as used for the FRP reinforcement of glulam beams [3]. Nine repetitions were undertaken. The cross-sectional areas of the specimens were measured prior to testing using a vernier caliper with precision to 0.01mm. After ensuring perfect vertical placement of the specimens in the tension machine, the specimen was clamped uniformly in the grips and an extensometer with 50mm gauge length was fitted to the tensile specimens prior to testing at a displacement speed of 0.033mm second. Testing was executed using a 250 kN Denison testing machine and tests were only carried out when conditions of 65±5% relative humidity and temperature of 20±2°C was present in the laboratory.

A modulus of elasticity in tension of 38.44GPa with standard deviation of 2.25GPa and ultimate tensile strength of 701MPa with standard deviations of 45GPa were determined for the FRP material. Values are of a lower magnitude than that specified by the manufacturer as testing involved two plates bonded together. The data determined for the FRP from this test programme was used in the finite element model simulations.

4 RESULTS

The results from the numerical simulations and experimentally tested unreinforced (Phase A) and reinforced beams (Phase B) are presented in the following sections. These beams formed part of a larger beam test programme discussed in [3] and so the unreinforced beams comprised Beam Numbers 1, 2, 3, 36, 37 and 38 and the reinforced beams comprised Beam Numbers 5, 11, 18, 24 and 31. The results from the parametric analysis, whereby the percentage of reinforcement was varied, are also given.

4.1 UNREINFORCED BEAMS

The load-deflection behaviour predicted by the finite element model and that of the experimentally tested unreinforced beams are shown in Figure 11 to Figure 16. Strong agreement is obtained between the predicted beam behaviour and experimental behaviour with both exhibiting linear elastic behaviour to failure. In general, the predicted stiffness from the finite element model marginally over-predicts that of the experimentally determined stiffness. Indentation at the supports during the experimental testing is believed to be one of the reasons for the differences between numerical predictions and the experimental results.

The ultimate moment capacity predictions obtained from the finite element models for Beam 1, Beam 2, Beam 36 and Beam 38 were conservative in relation to the experimentally tested beams. The predictions for Beam 2 (78.0%) and Beam 38 (72.4%) are particularly conservative and this is believed to be as a result of the laminating factor being significantly greater for glulam fabricated from C16 spruce as well as the low correlation coefficient associated with the in-grade tension testing programme. For two of the beams, Beam 3 and Beam 37, the ultimate moment capacity is over-predicted and this is believed to have occurred because of the relatively low correlation coefficient of 0.3867 between the tension strength of the timber and knot area ratio. With a more intensive in-grade tension test programme, a higher correlation coefficient could be established which would increase the accuracy of the predictions.

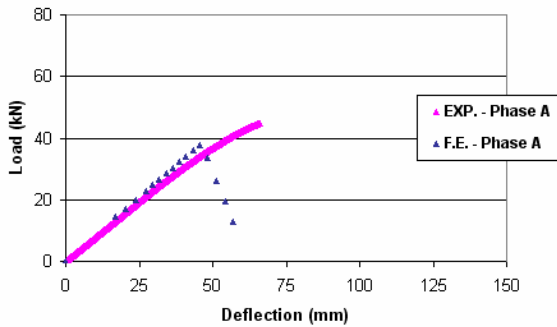


Figure 11: Unreinforced load-deflection curve (Beam 1)

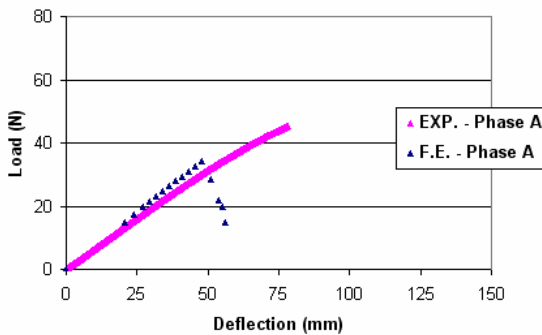


Figure 12: Unreinforced load-deflection curve (Beam 2)

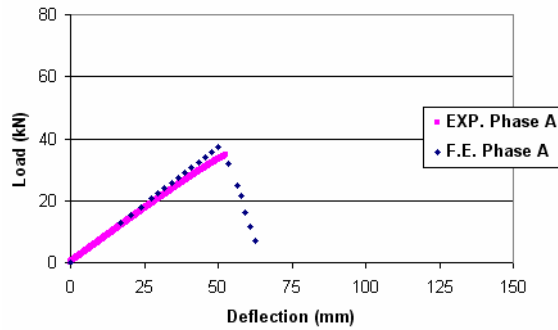


Figure 13: Unreinforced load-deflection curve (Beam 3)

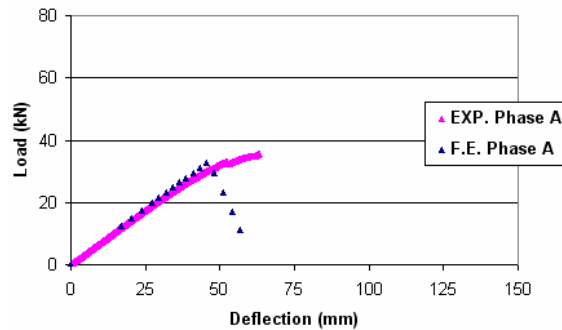


Figure 14: Unreinforced load-deflection curve (Beam 36)

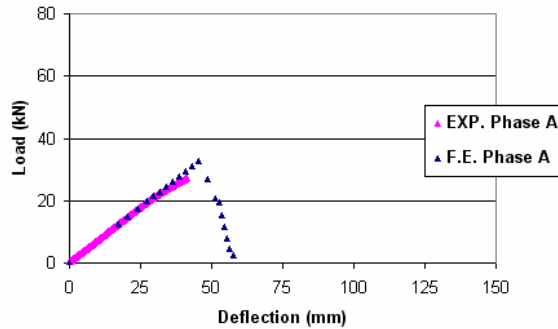


Figure 15: Unreinforced load-deflection curve (Beam 37)

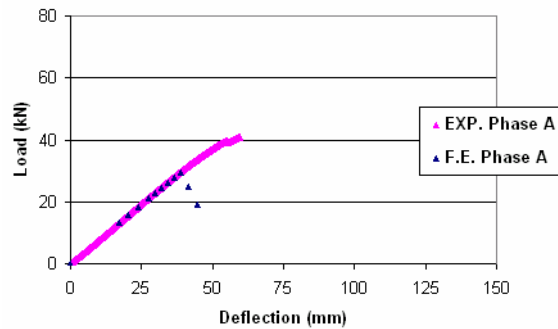


Figure 16: Unreinforced load-deflection curve (Beam 38)

4.2 REINFORCED BEAMS

Predicted load-deflection behaviour from the nonlinear finite element model is contrasted with the experimentally determined load-deflection behaviour for the reinforced beams in Figures 17 to Figure 21. For each of the five reinforced beams, simulations are undertaken to predict the behaviour of the beam in its unreinforced condition (Phase A) and the behaviour when failure occurs at the in-grade strength in the bottom tension lamination (Phase B (i)) as predicted from the relationships established in the material characterisation tests. The model demonstrates that enhancements in the stiffness, ultimate moment capacity and ductility of the section are obtained when the reinforcement is added. For Beam 18, a further analysis was undertaken to determine the response when the failure strength in the bottom lamination was taken as that associated with clear wood (Phase B (ii)). This value was determined from tension testing of clear wood specimens [13]. The extended nonlinear behaviour that is obtained (Figure 19) highlights the importance of eliminating significant defects from the more highly stressed tension zones. The finite element model marginally over-predicted the limit of proportionality for Beam 18 in comparison to the experimental behaviour. This is believed to be because of the low coefficient of determination associated with determination of the compressive strength of the timber in the top lamination. In general, the finite element model demonstrates strong agreement with the experimentally tested beams for predicting the pseudo-ductility associated with the load-deflection behaviour of the reinforced glulam beams.

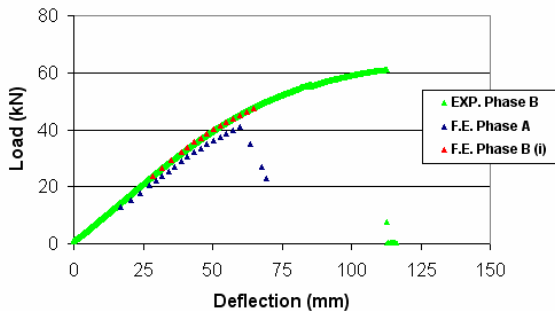


Figure 17: Reinforced load-deflection curve (Beam 5)

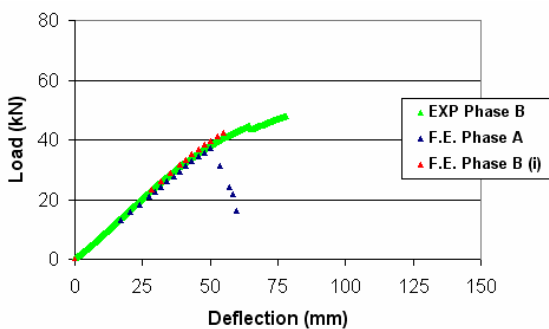


Figure 18: Reinforced load-deflection curve (Beam 11)

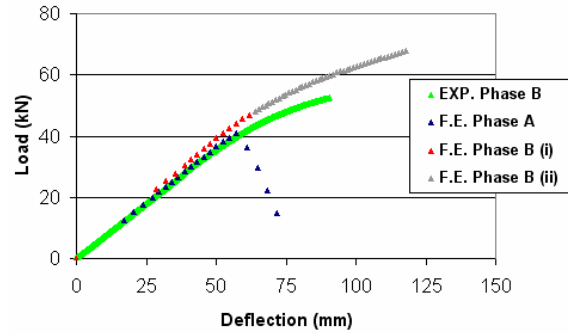


Figure 19: Reinforced load-deflection curve (Beam 18)

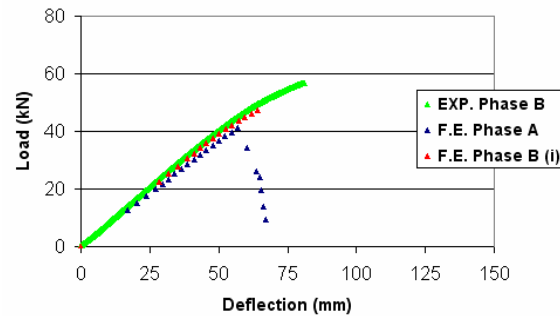


Figure 20: Reinforced load-deflection curve (Beam 24)

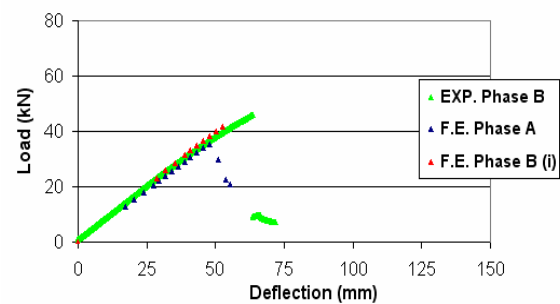


Figure 21: Reinforced load-deflection curve (Beam 31)

Comparisons of the stiffness and ultimate moment capacity results between the experimental testing and finite element model predictions are shown in Table 4 and Table 5, respectively. Good agreement is achieved between the two sets of results. For all five beams, the finite element model obtained a mean stiffness of 101.1% (with standard deviation of 3.5%) of the experimental test results. The finite element predictions of ultimate moment capacity are extremely satisfactory with a mean prediction percentage of 87.7% of the performance of the experimental test results being obtained. The model proved conservative for all five beams in the test phase and a standard deviation of 5.4% was associated with these results.

Table 4: Predicted EI versus experiment EI

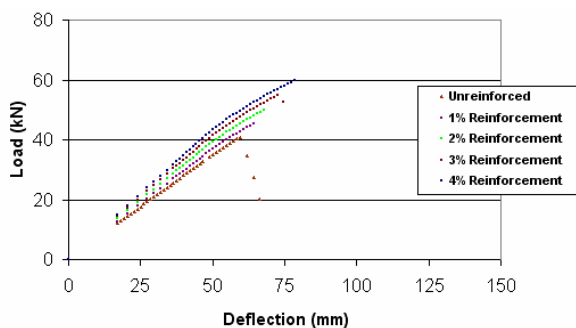
Beam	Experimental EI (Nmm ²)	Predicted EI (Nmm ²)	Predicted/Experimental (%)
Beam 5	5.72E+11	5.90E+11	103.2
Beam 11	5.71E+11	5.81E+11	101.6
Beam 18	5.35E+11	5.61E+11	104.8
Beam 24	5.86E+11	5.60E+11	95.6
Beam 31	5.74E+11	5.78E+11	100.6
Mean	5.68E+11	5.74E+11	101.1
Stdev.	1.92E+10	1.30E+10	3.5

Table 5: Predicted M_{ult} versus experimental M_{ult}

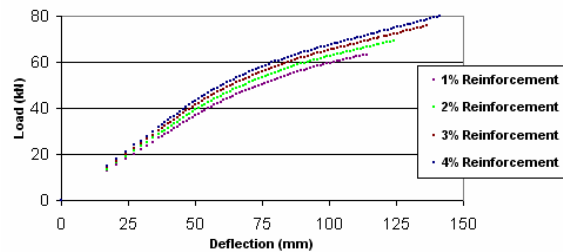
Beam	Experimental M _{ult} (kNm)	Predicted M _{ult} (kNm)	Predicted/Experimental (%)
Beam 5	34.37	27.04	78.7
Beam 11	27.30	24.14	88.4
Beam 18	29.95	27.45	91.6
Beam 24	32.43	28.36	87.4
Beam 31	25.74	23.71	92.1
Mean	29.96	26.14	87.7
Stdev.	3.55	2.08	5.41

4.3 PARAMETRIC ANALYSIS

The modelling work presented thus far has demonstrated that the behaviour of the experimentally tested beams can be predicted with good accuracy. It is therefore considered appropriate that the model can be used to undertake parametric analyses to determine the influence of increasing reinforcement percentages on the beam responses. The effect of increasing the reinforcement percentage of Fulcrum plate at the soffit of the reinforced beams is illustrated in Figure 22 with regard to the load-deflection behaviour.

**Figure 22: Influence of reinforcement percentage with in-grade failure (Beam 18)**

It is clear that with increasing reinforcement percentages, the non-linear behaviour of the section improves as does the stiffness and ultimate moment capacity. Similar improvements are predicted for the beams in which clear tension wood failure is examined (Figure 23).

**Figure 23: Influence of reinforcement percentage with clear wood failure (Beam 18)**

5 CONCLUSIONS

The development of a plane stress nonlinear finite element model for unreinforced low-grade glulam and FRP plate flexural reinforced glulam subject to four point bending is described. The model incorporates anisotropic plasticity theory for the timber laminations in the compression zone of the glulam beams. The failure model is based on the maximum stress criterion. Yield stresses for the timber in compression parallel to grain and the ultimate tension strength of the timber are determined from the relationships established from mechanical test programmes. In general, strong agreement is found between the simulated beam behaviour and the experimental testing of both the unreinforced and reinforced glulam beams. Ductile behaviour was predicted when FRP plate reinforcement was strategically located in the higher tension stressed zone of the beams as obtained in the experimental testing. Modest improvements in the stiffness were predicted with the addition of the FRP reinforcement with more considerable enhancements in the ultimate moment capacity obtained. The model can readily accommodate different spans, reinforcement percentages and material properties, and is therefore a useful tool to optimize the design of the FRP reinforced glulam beams. It was seen from a parametric analysis that as the reinforcement percentage is increased, the stiffness of the hybrid sections is enhanced, the ultimate moment capacity is augmented and increased ductility is achieved.

ACKNOWLEDGEMENT

The authors would like to express their sincere thanks to COFORD; National Council for Forest Research and Development, (Ireland), Coillte and the National University of Ireland, Galway for the financial support provided. The primary author would also like to thank the Irish Research Council, Science, Engineering and Technology (IRCSET) for sponsorship. The technical assistance provided by Rotafix Ltd. is appreciated.

REFERENCES

- [1] Thelandersson S, Larsen HJ. Timber Engineering, Wiley & Sons, London, 2003.
- [2] Hollaway LC, Teng JG. Strengthening and rehabilitation of civil infrastructures using fibre-reinforced polymer (FRP) composites, Woodhead Publishing Ltd. 2008.
- [3] Alam, P. The reinforcement of timber for structural applications and repair, PhD thesis, Dept. of Mechanical Engineering. University of Bath, U.K. 2004.
- [4] Raftery G, Harte A, Low-grade glulam reinforced with FRP plate, Composites Part B: Engineering. Submitted for publication.
- [5] EN 408, Timber structures - structural timber and glued laminated timber – determination of some physical and mechanical properties, 2003.
- [6] Raftery G, Harte A, Rodd P. Bonding of FRP materials to wood using thin epoxy gluelines. Int. J. Adhes Adhesv. 29 (5): 580-588, 2009.
- [7] I.S. 127 – Structural timber – Visual strength grading – Sawn softwoods with rectangular cross section, N.S.A.I., 1 Swift Square, Northwood, Santry, Dublin 9, Ireland, 2002.
- [8] Falk, R.H., Solli, K.H., Aasheim, E. The performance of glued laminated beams manufactured from machine stress graded Norwegian spruce, Report No. 77, Norwegian Institute of Wood Technology, Oslo, 1992.
- [9] Falk, R.H., Colling, F. Laminating effects in glued laminated timber beams, Journal of Structural Engineering, 121 (12): 1857-1863, 1995.
- [10] Bodig, J., Jayne, B.A. Mechanics of wood and wood composites, Krieger publishing company, Malabar, Florida, U.S.A., 1993.
- [11] Dinwoodie, J.M. Timber: Its nature and behaviour, 2nd Edition, Taylor and Francis, 2000.
- [12] EN 2747, Glass fibre reinforced plastics – Tensile test, 1998.
- [13] BS 373, Methods of testing of small clear specimens of timber, 1957.